Predicting Resistance Spot Weld Failure Modes in Shear Tension Tests of Advanced High-Strength Automotive Steels

To judge the quality of resistance spot welds in advanced high-strength steels, the load-bearing ability of the weld should be considered more important than the fracture mode

BY D. J. RADAKOVIC AND M. TUMULURU

ABSTRACT. Finite element modeling and fracture mechanics calculations were used to predict the resistance spot weld failure mode and loads in shear-tension tests of advanced high-strength steels (AHSS). The results were compared to those obtained for an interstitial-free (IF) steel. The results of the work confirmed the existence of a competition between two different types of failure modes, namely full button pullout and interfacial fracture. The force required to cause a complete weld button pullout-type failure was found to be proportional to the tensile strength and the thickness of the base material as well as the diameter of the weld. The force to cause an interfacial weld fracture was related to the fracture toughness of the weld, sheet thickness, and weld diameter. For high-strength steels, it was determined that there is a critical sheet thickness above which the expected failure mode could transition from pullout to interfacial fracture. In this analysis it was shown that, as the strength of the steel increases, the fracture toughness of the weld required to avoid interfacial failure must also increase. Therefore, despite higher load-carrying capacity, due to their high hardness, the welds in high-strength steels may be prone to interfacial fractures. Tensile testing showed that the load-carrying capacity of the samples that failed via interfacial fracture was found to be more than 90% of the load associated with a full button pullout. This indicates that the load-bearing capacity of the welds is not affected by the fracture mode. Therefore, the mode of failure should not be the only criteria used to judge the quality of spot welds. The load-bearing capacity of the weld should be the primary focus in the evaluation of the shear-tension test results in AHSS.

D. J. RADAKOVIC and M. TUMULURU are with the Research and Technology Center, United States Steel Corp., Munhall, Pa.
Based on a paper presented at the 2006 FABTECH International & AWS Welding Show, Atlanta, Ga.

Introduction

The use of advanced high-strength steels (AHSS), such as dual-phase and transformation-induced plasticity (TRIP) steels, has been steadily increasing over the past few years in automotive applications (Refs. 1, 2). This is due to the advantages that AHSS grades offer, in terms of higher strength that enables the automakers to decrease the vehicle weight for improved fuel economy and improved crash energy absorption for better occupant protection. The two grades of AHSS that have seen increased use in automobiles are the dual-phase and TRIP steels. The steel grades that are used commercially in automotive bodies at present are those with minimum strength levels of 500, 590, and 780 MPa. Resistance welding is the predominant mode of fabrication in automotive production with a typical vehicle in North America containing about 4000 to 5000 welds. Therefore, good resistance spot welding behavior is one of the key characteristics of any steel grade to be considered for use in automobile body production.

Several tests are generally used to characterize the resistance spot welding behavior of steels. These include the welding current range determination, metallographic characterization of the weld and heat-affected zone microstructures, microhardness, and weld tensile tests (Ref. 3). One type of weld tension test typically done is called the shear-tension test (sometimes referred to as lap-shear test). In this test, two sheet samples, 140 mm long by 60 mm wide are overlapped by 45 mm and joined with a single spot weld located at the center of the overlapped region — Fig. 1. The sample is then pulled in tension. Due to the offset of the sheets, the application of tension creates a bending moment that causes rotation of the weld nugget. This type of deformation is demonstrated with a finite element simulation — Fig. 2. For clarity, only one half of the model is shown. The combination of bending and shear loading that results from this deformation causes a complicated stress pattern to develop in and around the nugget.

There are two different failure modes that are generally observed in shear-tension tests, namely, "interfacial fractures" and "full button pullout" — Fig. 3. In the interfacial fracture, the weld fails at the interface of the two sheets, leaving half of the weld nugget in one sheet and half in the other. In the full button pullout, fracture occurs in the base metal or in the weld heat-affected zone at the perimeter of the weld. In this failure mode, the weld nugget is completely torn from one of the sheets with the weld remaining intact. It is also possible to get a combination of the two failure modes in which a portion of the nugget is pulled out of one of the sheets and the rest of the nugget shears at the interface.

A review of the literature showed that considerable work has been done to understand the behavior of spot welds under tensile and shear loading. Work done by Davidson and Imhof (Refs. 4–6) showed that spot weld strength in the shear-tension test is related to the stiffness of the joint. They found that, for stiffer test specimens the degree of rotation that the spot

KEYWORDS

Dual-Phase Steels
TRIP Steels
Fracture Mechanics
Finite Element Modeling
Shear-Tension Test
Failure Mode

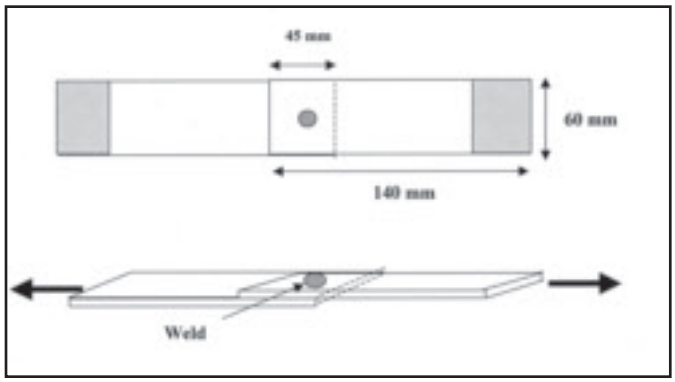

Fig. 1 — Sketches showing the dimensions of a shear-tension test coupon. The arrows in the bottom sketch show the direction of the application of tensile load during the test.

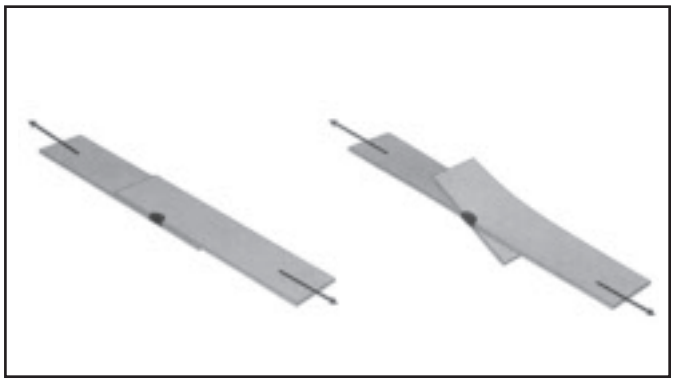

Fig. 2 — Sketches showing half sections of a shear-tension coupon before (left) and after (right) the application of load. Bending of the sample (shown in the right-side sketch) results from the offset of the sheets.

weld undergoes becomes smaller, which in turn, leads to increased joint strength. Davidson and Imhof correlated the joint strength with weld nugget rotation but did not offer a relationship for the stress intensity at the weld. Pook (Ref. 7) developed a relationship for the stress intensity at the weld nugget based on analytical solutions. Pook showed that the weld diameter and sheet thickness have an effect on the stress intensity at the nugget perimeter. Chao (Ref. 8) studied the expected failure modes and failure loads for spot welds based on assumed stress distributions around the perimeter of the weld resulting from a combination of shear and tensile loading. Radaj and Zhang (Ref. 9) and Zhang (Ref. 10) performed detailed finite element modeling of spot welds under shear tension load to predict the stress intensity around the weld. This analysis suggested that correlations and trends predicted in earlier work did not correlate well with the detailed computer models. Radaj and Zhang developed some simplified equations to predict the stress intensity of spot welds in various tests, including the shear-tension test. The correlations were consistent with the computer simulations. However, the simulations are computationally intensive and time consuming.

In the evaluation of the shear-tension test results in spot welds, it is generally believed in the automotive industry that an interfacial shear failure is indicative of poor weld integrity. This has generally been true for low-strength steels (tensile strength equal to or less than 300 MPa), in which interfacial failure is normally associated with insufficient fusion or some sort of a weld imperfection, such as gross porosity. However, it is not clear if interfacial fractures in shear-tension tests indicate poor weld integrity in AHSS grades. With the increased use of these steels in automotive bodies, it is important to study their fracture behavior in shear-tension tests so that welds, otherwise sound, do not get rejected solely based on fracture appearance. Furthermore, an understanding of the fracture behavior may allow the automotive companies to use these steels and enable them to take advantage of the benefits that these steel grades offer. Additionally, the tensile fracture behavior of the recently introduced advanced high-strength steels, such as dual-phase and TRIP steels, has not been reported previously. Therefore, a study was undertaken to examine and predict the fracture modes possible in shear tension tests in dual-phase steels with a minimum tensile strength of 590 and 780 MPa and TRIP steel with a minimum tensile strength of 780 MPa. An attempt based on finite element modeling (FEM) and fracture mechanics calculations on data collected from actual shear-tension tests was made to predict the resistance spot weld failure modes in shear-tension tests.

Table 1 — Welding Conditions

Welding Machine Manufacturer	Taylor Winfield Corp.
Welding Machine Type	Pedestal-type
Welding Machine Transformer	100 kVA
Welding Controller	TrueAmp IV
Electrode Face Diameter	6 mm
Electrode Force	For IF Steel: 3.1 kN (697 lbf) For AHSS Grades: 4.2 kN (945 lbf) for 1 mm 5.4 kN (1200 lbf) for 1.2 and 1.6 mm
Squeeze Time	75 cycles
Weld Time	13 cycles (for 1-mm sheets) 14 cycles (for 1.2-mm sheets) 18 cycles (for 1.6-mm sheets)
Hold Time	10 cycles
Preheating	None
Postheating	None
Electrode Coolant Water Temperature	21°C
Tip Cooling	3.7 L/min (1 gal/min)

Materials and Experimental Procedure

Dual-phase steel coils with a minimum ultimate tensile strength of 590 and 780 MPa, transformation-induced plasticity

Table 2 — Material Properties Used

Steel Grade	Yield Strength, MPa	Tensile Strength, MPa	Elongation, %
IF	137	302	45
590 Dual Phase	370	650	25
780 Dual Phase	470	805	19
780 TRIP	440	844	24

Note: Elastic Modulus of 207 GPa and Poisson's Ratio of 0.29 used for each case.

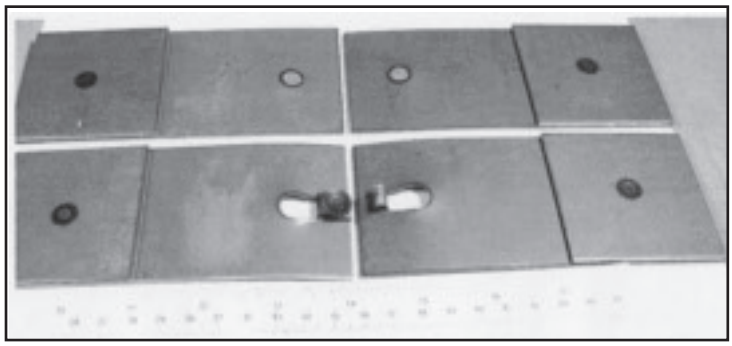

Fig. 3 — A photograph of two shear-tension test samples showing the two different weld fracture morphologies described in the text. The sample on the top showed interfacial fracture, and the sample on the bottom showed full button pullout. The spot welds on both ends of each sample were made to attach shims for tensile testing.

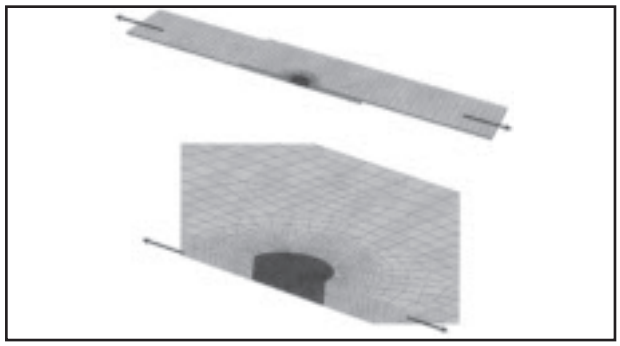

Fig. 4 — Schematic showing a three-dimensional finite element model of spot weld shear-tension test sample. The lower picture shows a close-up view of the mesh in the vicinity of the spot weld. Sheet thickness is 1.0 mm and button size is 6 mm.

(TRIP) steel with a minimum tensile strength of 780 MPa, and interstitial-free (IF) steel with a tensile strength of 300 MPa were used in the study. The IF steel was used because it is extensively used for body panels in automobile bodies and the automotive industry is quite familiar with its welding and fracture behaviors. Therefore, it would be a good candidate to provide a comparison for the fracture behavior of AHSS grades.

All the coils were coated with 42/42 g/m^2 (42 g/m^2 on each side) hot-dipped galvanneal (HDGA) coating. Coatings are generally applied to steel sheets used in the automotive industry for corrosion protection. A galvanneal coating is obtained by heating the zinc-coated steel at 450°–590°C (840°–1100°F) immediately after the steel exits the molten zinc bath. The nominal HDGA coating weights for the coils used were 42/42 g/m^2. These coating weights are typical of current commercial automotive use. All the coils used were melted, hot and cold rolled at United States Steel Corp. — Gary Works and coated subsequently at PRO-TEC Coating Co. of Leipsic, Ohio. The coils ranged in thickness from 1 to 2 mm.

Nominally, the dual-phase and TRIP steels contain about 0.09 to 0.14 wt-% carbon and are generally alloyed with various amounts of manganese, chromium, and molybdenum to achieve the required tensile strength (Refs. 11, 12). In addition to these alloying elements, TRIP steels typically contain silicon or aluminum to effectively suppress the formation of cementite by increasing the time required for its formation and lowering its thermodynamic stability (Ref. 12).

Tensile test samples were prepared from coils in the as-received condition without any cleaning of the mill oil used prior to shipping the coils. Weld shear-tension tests were conducted per Ref. 3. The current required to produce a weld button size equal to or 90% of the face diameter of the electrode tip used was determined. This was done using the highest current possible without causing expulsion in the samples. The welding parameters used for making the test samples are shown in Table 1. Load to failure and the weld fracture morphology were noted in each case. In each case, five tensile samples were tested and the average values reported.

In order to better understand the sample behavior and failure modes that occur in the shear-tension test, finite element computer simulations of this test were performed. The modeling was done using *ABAQUS* Version 6.5 general-purpose finite element modeling (FEM) software. The simulations were run on a Silicon Graphics Octane 2 workstation. Three-dimensional models of the test sample were developed using eight-node brick elements. Model strain predictions were found to converge for a local element size near the weld that is less than 25% of the sheet thickness for each of the three thicknesses evaluated. An example of a finite element model of the shear-tension test sample for a 1-mm sheet with a 6-mm button is shown in Fig. 4. The lower picture in Fig. 4 shows a close-up view of the mesh in the vicinity of the spot weld. In order to reduce computation time, symmetry conditions were applied so that only one half of the sample had to be represented. In the study, several models were developed to represent different sheet thicknesses and weld diameters.

The stress-strain behaviors of the three types of steel grades used in the simulations are shown in Fig. 5. The computer modeling software allows for the definition of elastic as well as plastic behavior of materials and the appropriate data points were defined to describe the load dis-

Table 3 — Results of Simulations for Interstitial-Free Steel Samples (Ultimate Tensile Strength = 300 MPa)

Weld Diameter (mm)	Nominal Sheet Thickness (mm)	FEM Failure Mode[a]	FEM Failure Load (N)	K-Factor IF or PO
2.5	1.0	IF	1200	0.62
5.0	1.0	PO	3640	2.32
7.5	1.0	PO	5400	2.30
10	1.0	PO	7070	2.26
2.5	1.5	IF	1200	0.61
5.0	1.5	IF	4720	0.60
7.5	1.5	PO	8140	2.31
10	1.5	PO	10700	2.28
2.5	2.0	IF	1200	0.61
5.0	2.0	IF	4540	0.58
7.5	2.0	IF	10280	0.58
10	2.0	PO	13920	2.22
13	2.0	PO	16700	2.17

(a) IF – interfacial fracture; PO – full button pullout fracture.

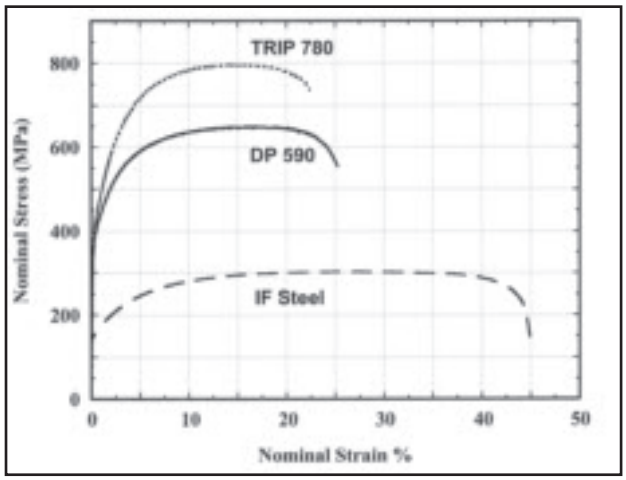

Fig. 5 — Stress-strain curves for the three steel grades used in the study.

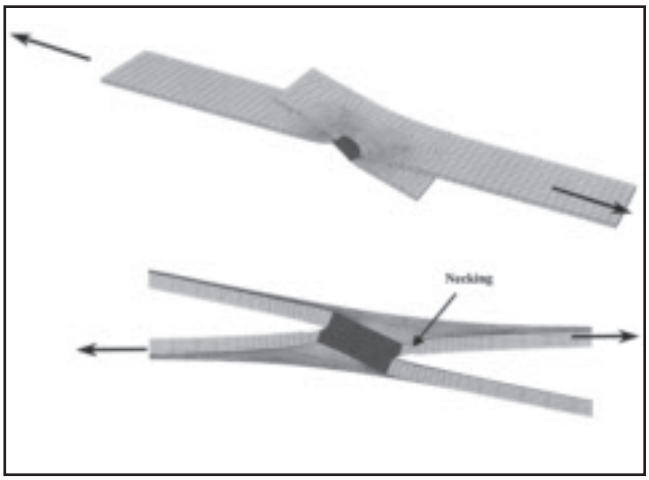

Fig. 6 — Model-predicted deformation around the weld nugget in the shear-tension test at the onset of a full button pullout failure. Sheet thickness is 1.0 mm and button size is 6 mm.

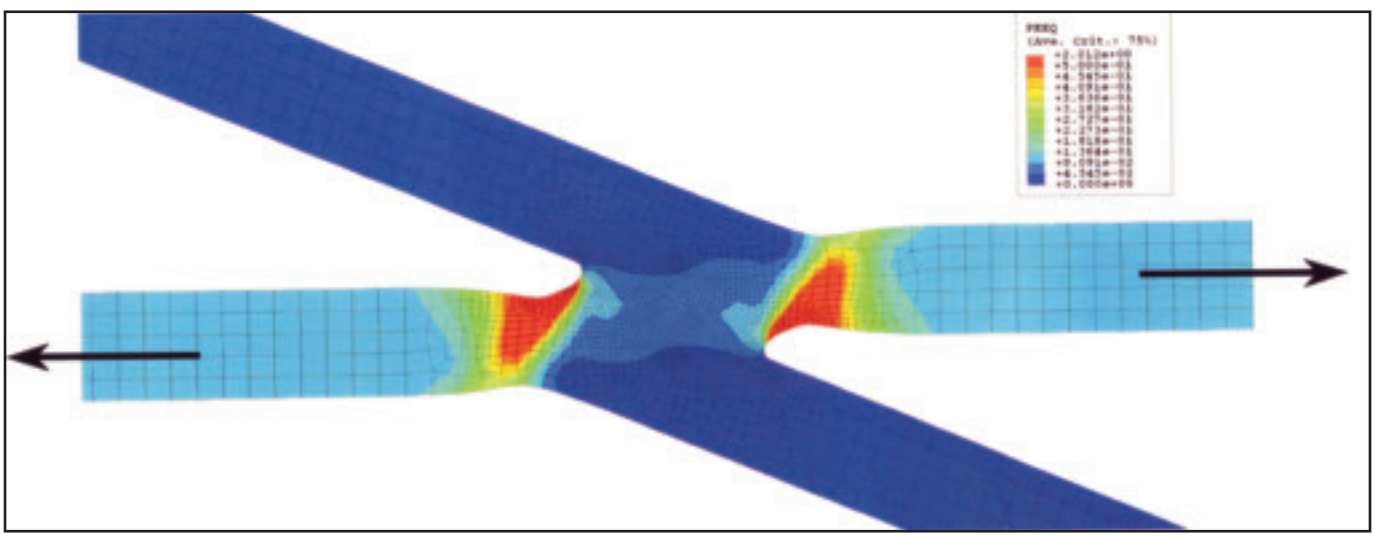

Fig. 7 — Close-up view of the model-predicted plastic strain distribution that occurs during a full button pullout failure in the shear-tension test. Note the necking of the base metal immediately outside the weld nugget.

placement behavior shown in Fig. 5. The material properties defined in the analysis are shown in Table 2.

As a starting point in the study, the properties of the entire test specimen were considered to be homogeneous. It was assumed that the properties of the weld and the heat-affected zone were the same as those of the base metal. The homogeneous model was used only to estimate loads required for pullout failure. This assumption was made to examine the effect of button size and sheet thickness on the behavior of the weld in this test.

To predict the failure loads associated with interfacial fracture, additional considerations were made. It was observed that the interfacial failures initiated at the notch created at the sheet interface at the periphery of the weld. This suggested that the fracture toughness of the weld and heat-affected zone controlled the failure mode and load. Previous work (Ref. 10) provided a means to estimate the stress intensity at the root of the notch at the sheet interface and is described in later sections.

In the analysis, sheet thicknesses of 1.0, 1.5, and 2.0 mm were simulated. For each sheet thickness, four or five different weld sizes were modeled ranging in diameter from 2.5 to 13 mm. For all models, the sample length and width were held constant. A total of 39 simulations were run, 13 for each of the three steel types, namely IF, dual-phase, and TRIP steels.

In all models, one end of the sample was held fixed and an applied axial displacement was applied to the opposite end. The reaction force was monitored as a function of the applied displacement. When the failure strain was reached in either the weld or the base metal outside the weld, failure was assumed to have occurred. The magnitude of the reaction force at the point when failure strain was reached was considered to be the load-carrying capacity of the sample.

Results and Discussion

The results of the analyses of the homogeneous shear-tension test samples are shown in Tables 3–5 and in Figs. 6–11. Figure 6 shows the model-predicted deformation of a sample at the onset of a pullout failure. In this failure mode, the strength of the material outside the weld

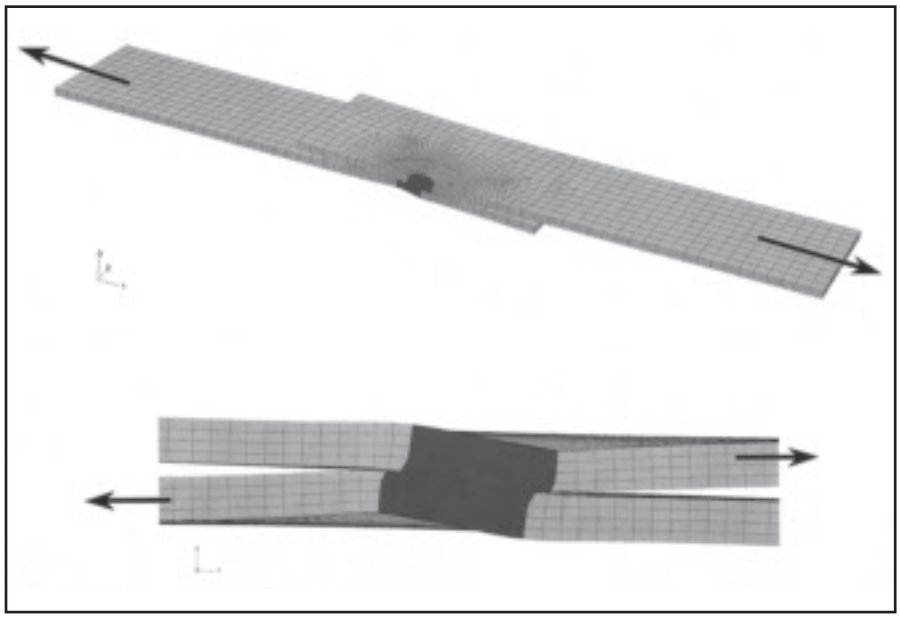

Fig. 8 — Mode-predicted deformation in the shear-tension test showing shear overload of the weld metal at the interface of the two sheets. Sheet thickness is 1.0 mm and button size is 4 mm.

nugget is exceeded and necking begins to occur at the location shown. After failure of the material at this location, the weld button is peeled out of the base metal around the weld perimeter. A more detailed model of this mechanism is shown in Fig. 7, which is a contour plot of the plastic strain in the homogeneous sample. As the figure shows, the maximum plastic strain is concentrated outside the weld nugget, which leads to necking and failure at this location. The predicted deformation that occurs during the interfacial failure is shown in Fig. 8. Nearly all of the strain is concentrated in the weld at the interface of the two sheets. Figure 9 shows the plastic strain distribution associated with the interfacial failure. There is some strain outside the weld nugget, but shear failure of the weld occurs before the pullout failure can initiate. These results are shown in graphical form in Fig. 10. The maximum plastic strain in the weld at the interface of the sheets and the maximum strain in the base metal outside the weld nugget are plotted as a function of the applied end displacement. For the case of full button pullout, the strain in the base metal outside the weld nugget is greater than that developed at the weld interface and the opposite is true for the case of the weld interfacial failure. Based on these results, it is apparent that there is a competition between the pullout and the interfacial failure modes

Table 4 — Results of Simulations for DP 590 Steel (Minimum Ultimate Tensile Strength = 590 MPa)

Weld Diameter (mm)	Nominal Sheet Thickness (mm)	FEM Failure Mode[a]	FEM Failure Load (N)	K-Factor IF or PO
2.5	1.0	IF	2290	0.55
5.0	1.0	PO	7600	2.27
7.5	1.0	PO	11600	2.31
10	1.0	PO	15060	2.25
2.5	1.5	IF	2260	0.54
5.0	1.5	IF	9660	0.58
7.5	1.5	PO	16860	2.24
10	1.5	PO	22700	2.26
2.5	2.0	IF	2300	0.55
5.0	2.0	IF	9300	0.56
7.5	2.0	IF	22150	0.59
10	2.0	PO	28700	2.14
13	2.0	PO	35500	2.12

(a) IF – interfacial fracture; PO – full button pullout fracture.

For the pullout failure, the results of the finite element simulations showed that there was a strong correlation between failure load and the material strength, sheet thickness, and weld diameter. The load to cause interfacial failure was found to be more strongly dependent on the weld diameter and less on the sheet thickness. The predicted failure loads were found to adhere to the following correlations:

$$F_{PO} = k_{PO} \cdot \sigma_{UT} \cdot d \cdot t \qquad (1)$$

$$F_{IF} = k_{IF} \cdot \sigma_{UT} \cdot d^2 \qquad (2)$$

Where F_{PO} is the failure load for pullout failure, F_{IF} is the failure load for interfacial fracture, σ_{UT} is the tensile strength of the material, d is the weld diameter, and t is the sheet thickness. Equations 1 and 2 were derived based on the fact that the force required to cause failure is equal to the product of the strength of the material and the failed area of cross section. In this analysis, the material was assumed to be homogeneous. Therefore, the strength of the weld and the base metal are both equal to σ_{UT}. In Equations 1 and 2, k_{PO} and k_{IF} were constants determined from the modeling.

The results of the analysis of the homogeneous sample analysis are shown in Tables 3–5. Each table corresponds to a different steel type (IF, DP, and TRIP) and shows the combinations of sheet thickness and weld diameter that were simulated. As predicted in Equations 1 and 2, the failure loads to cause pullout were found to be proportional to the weld diameter and the sheet thickness while those for interfacial failure were proportional to the square of the weld diameters. The predicted failure mode and failure load as well as the constant k_{PO} or k_{IF} are shown in the tables. The values for k_{PO} and k_{IF} were backcalculated from Equations 1 and 2 by using the model-predicted failure loads, weld diameters, sheet thicknesses, and base metal strengths. The fact that the values of these two constants were fairly consistent for each case (k_{PO}~2.2 and k_{IF}~0.6) indicates that Equations 1 and 2 are good estimates of the model-predicted failure mode (for the homogeneous samples that were simulated).

Examination of Figs. 6–9 showed that, due to offset of the sheets, the shear-tension test specimens undergo rotation along an axis perpendicular to the loading direction. The degree of rotation was found to be greater for the cases of full button pullout failures (Figs. 6, 7) compared to those that failed interfacially (Figs. 8, 9). Davidson and Imhof (Ref. 6)

discussed the significance of specimen rotation during fatigue testing of spot welded samples. In fatigue testing, shear-tension test coupons are subjected to repeated tensile loads in the same manner as in static shear-tension testing. Davidson and Imhof showed that the stiffness of test samples affected the degree of rotation and that the weld failure mode was affected by the degree of rotation. They observed that stiffer samples (less rotation) failed interfacially, whereas, below a certain critical stiffness, the samples failed in the base metal and the weld remained intact.

Equations 1 and 2 are plotted graphically in Fig. 11 for dual-phase 590 steel and show the predicted interfacial and pullout failure load as a function of weld diameter. In this plot, the sheet thickness was assumed to be 1.5 mm and the sheet tensile strength equal to 590 MPa. A sheet thickness of 1.5 mm was chosen because it represented the mid-thickness of the normal range of steels (1 to 2 mm) used in automotive bodies. The minimum allowable tensile strength of the steel (590 MPa) was used for this case. According to the analysis, the lower of the two predicted failure loads will determine the mode of failure that occurs. Thus, the point where the two curves intersect indicates where the failure mode changes. The figure shows that, for this sheet thickness and strength, interfacial failures were predicted to occur for weld diameters below 6 mm and pullout failures for diameters greater than 6 mm. Figure 11B shows a similar plot with the exception that the weld diameter was assumed to be constant at 7 mm and the failure loads are plotted as a function of sheet thickness. These results indicate that pullout failures are more likely to occur on thinner sheet samples, and the mode can change to interfacial when the sheet thickness reaches a critical value (for this example ~ 1.7 mm). By setting Equations 1 and 2 equal to each other, the ratio of the weld diameter to the sheet thickness is determined to be roughly equal to 4. This suggests, for a homogeneous test sample, pullout failures will occur if the weld diameter is greater than four times the sheet thickness. Likewise, for a given weld diameter, the sheet thickness has to be less than 25% of the weld diameter for pullout to occur.

The homogeneous model predictions agreed well with the test data for cases where pullout failures occurred. This is because the pullout failures most often initiated in the base metal outside of the notch at the perimeter of the weld. A comparison of the actual failure loads and model-predicted failure loads for samples that failed via pullout is shown in Fig. 12. However, when comparing the homogeneous model results to actual test data, the predicted failure loads for the interfacial fractures were not consistent — Fig. 12. It was theorized that there were two main reasons for the differences. First, the model assumed that the sample was homogeneous. In reality, the mechanical properties of the weld, base metal, and different parts of the heat-affected zone are significantly different. For example, it was shown that the hardness of weld fusion zones and the heat-affected zones are much higher than those of the base material in dual-phase steels (Ref. 13). Further, the computer models did not account for the stress intensity at the perimeter of the weld. The model considered that the weld would fail when the strength of the weld metal is exceeded at the interface of the two sheets. This would more closely represent a shear overload of the weld metal rather than a fracture of the weld nugget initiating at the notch around the perimeter of the nugget.

A fracture mechanics study by Zhang (Ref. 9) provided an estimate of the stress intensity at the perimeter of the spot weld specifically for the shear-tension test. Fracture mechanics theory provides a means to evaluate the load-bearing ability of materials that have cracks or flaws. In fracture theory, the fitness for service of a structural member that contains a crack is determined by comparing the predicted stress intensity at the crack tip to the fracture toughness of the material. Like material properties such as tensile strength and elongation, fracture toughness is a material property that is determined from testing. Fracture analysis of a cracked member (in which stress intensity is compared to fracture toughness) is analogous to the analysis of notch-free structural members in which predicted stresses are compared to the strength of the material. Zhang's analysis yielded the following relationship for the stress intensity at the perimeter of the weld in the shear-tension test.

$$K_{eq}^{ts} = 0.694 \cdot \frac{F}{d\sqrt{t}} \qquad (3)$$

$$F_{IF} = 1.44 \cdot K_C \cdot d \cdot \sqrt{t} \qquad (4)$$

In Equation 3, K^{ts}_{eq} is the equivalent stress intensity factor at the spot weld, F is the applied load, d is the weld diameter, and t is the sheet thickness. Some actual test results are shown in Table 6. The table lists the steel grades, weld dimensions, failure mode, failure load, and the calculated

Table 5 — Results of Simulations for Dual-Phase and TRIP 780 Steels (Minimum Ultimate Strength = 780 MPa)

Weld Diameter (mm)	Nominal Sheet Thickness (mm)	FEM Failure Mode[a]	FEM Failure Load (N)	K-Factor IF or PO
2.5	1.0	IF	3000	0.58
5.0	1.0	PO	8950	2.17
7.5	1.0	PO	13600	2.20
10	1.0	PO	17780	2.15
2.5	1.5	IF	3030	0.59
5.0	1.5	IF	11900	0.58
7.5	1.5	PO	20500	2.21
10	1.5	PO	26400	2.13
2.5	2.0	IF	2920	0.57
5.0	2.0	IF	11530	0.56
7.5	2.0	IF	26760	0.58
10	2.0	PO	34760	2.11
13	2.0	PO	43700	2.12

(a) IF – interfacial fracture; PO – full button pullout fracture.

Table 6 — Actual Test Results and Predicted Stress Intensity at Failure

Material	Nominal Sheet Thickness (mm)	Weld Diameter (mm)	Failure Mode IF or PO	Failure Load (N)	Stress Intensity (N/mm$^{3/2}$)
780 DP	1.2	7.0	IF	14230	1294
590 DP	1.0	6.0	IF	9790	1126
780 TRIP	1.6	8.5	IF	21800	1385
780 DP	1.2	7.0	PO	15520	1411
780 DP	1.6	8.0	PO	22900	1581

(a) IF – interfacial fracture; PO – full button pullout fracture.

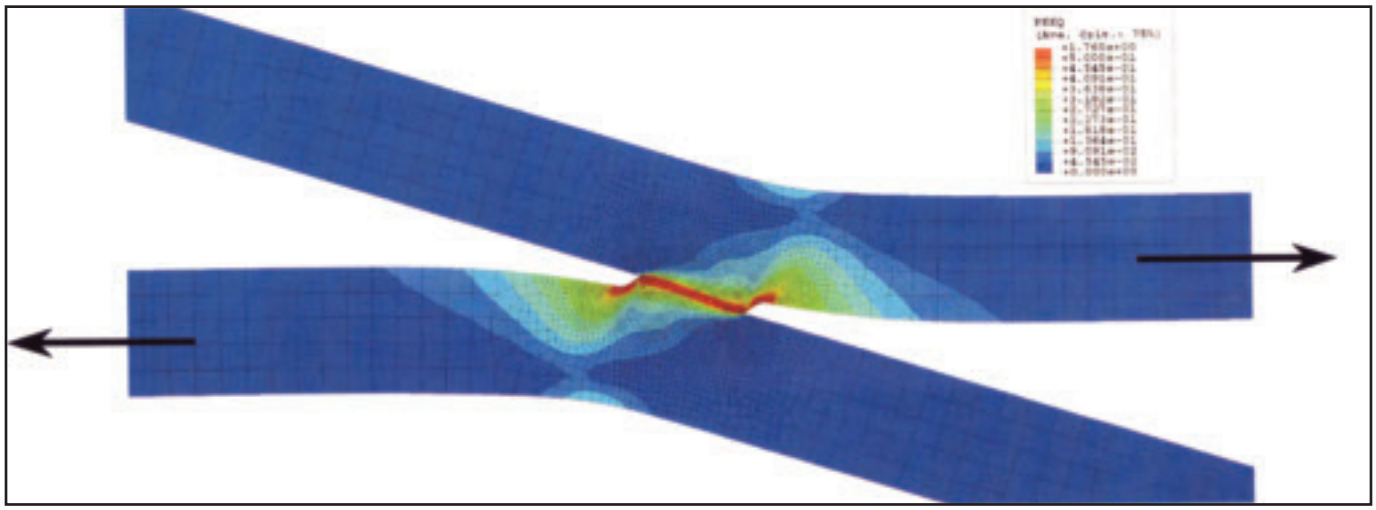

Fig. 9 — Close-up view of the model-predicted plastic strain distribution that occurs during a shear overload of the weld in the shear-tension test.

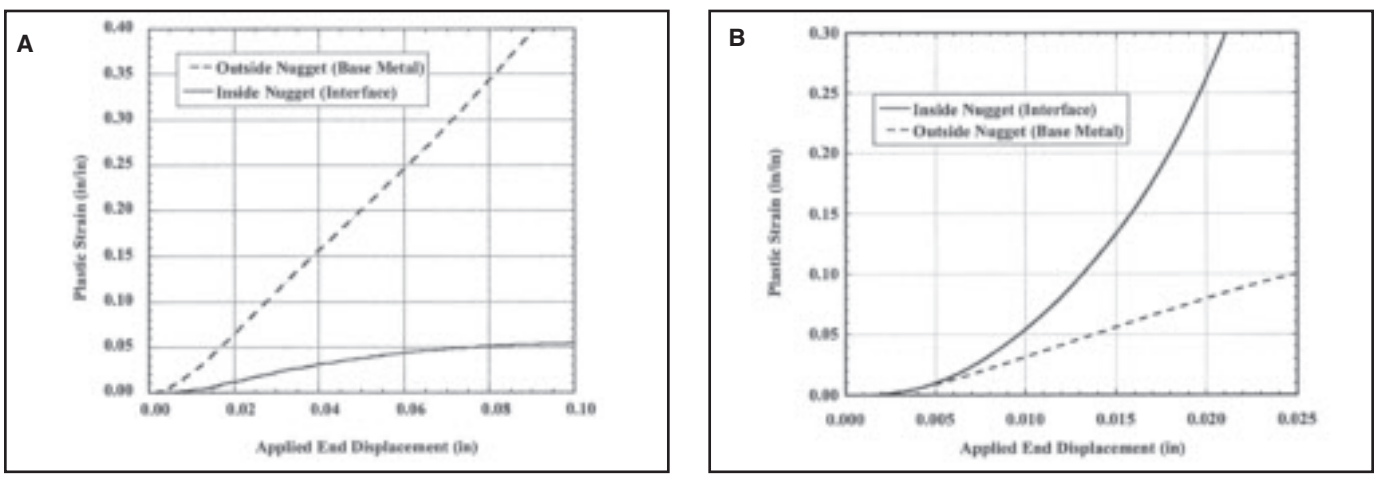

Fig. 10 — Predicted maximum plastic strain in the weld and in the base metal immediately outside the weld as a function of applied displacement in the shear tension test. There is a competition between pullout (A) and interfacial (B) modes of failure. Sheet thickness is 1.0 mm for both cases. The weld button size is 6 mm (A) and 4 mm (B).

stress intensity at failure. The stress intensities were calculated using Equation 3. The first three samples listed in the table failed via interfacial fracture. This suggests that the listed stress intensity at the time of failure is comparable to the fracture toughness of the weld. The stress intensities for the samples that failed via button pullout are also shown. For these two cases, the fracture toughness of the weld was apparently high enough to avoid interfacial fracture (i.e., the fracture toughness was greater than the values listed for the stress intensity when the pullout failure occurred).

Table 7 shows additional data comparing the model predictions to measured data. The table lists the steel grades, weld diameter, sheet thickness, actual failure load, and mode as well as the predicted failure load had pullout failures occurred

Table 7 — Comparison of Actual Shear Tension Test Results and Model Predictions

				Actual Test Data		Model Predictions	
Material	Sheet Thickness (mm)	Weld Diameter (mm)	Failure Mode[a]	Failure Load (N)	FEM Failure Mode	FEM Failure Load (N)	Percent of Max PO Load[b]
780 DP	1.2	7.5	PO	15500	PO	15820	—
780 DP	1.6	8.3	PO	22900	PO	23250	—
590 DP	1.0	7.0	IF	9900	PO	10340	96
780 DP	1.2	7.5	IF	14680	PO	15820	93
780 TRIP	1.6	8.5	IF	22060	PO	24330	91

(a) IF — interfacial fracture; PO — full button pullout.
(b) Ratio of the actual failure load to the model-predicted pullout failure load if the failure were to occur by the pullout mode (multiplied by 100).

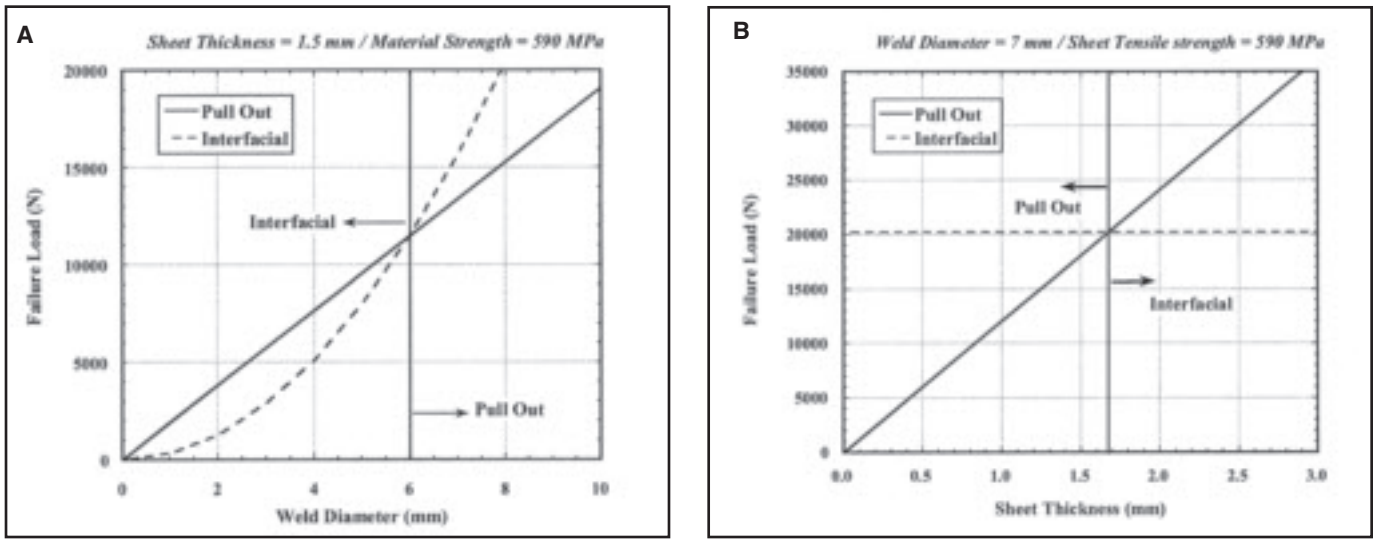

Fig. 11 — Predicted failure load in the analysis of the homogeneous shear-tension test sample as a function of the following: A — Weld diameter; B — sheet thickness.

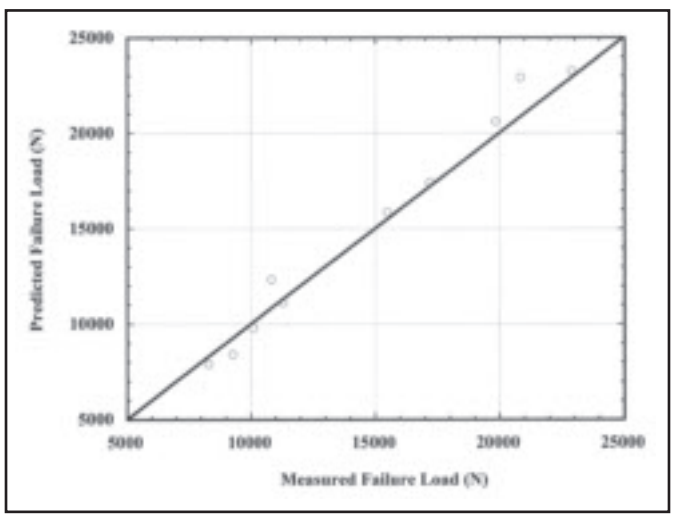

Fig. 12 — Comparison of actual failure loads to model-predicted failure loads in the shear-tension test for samples that failed via full-button pullout.

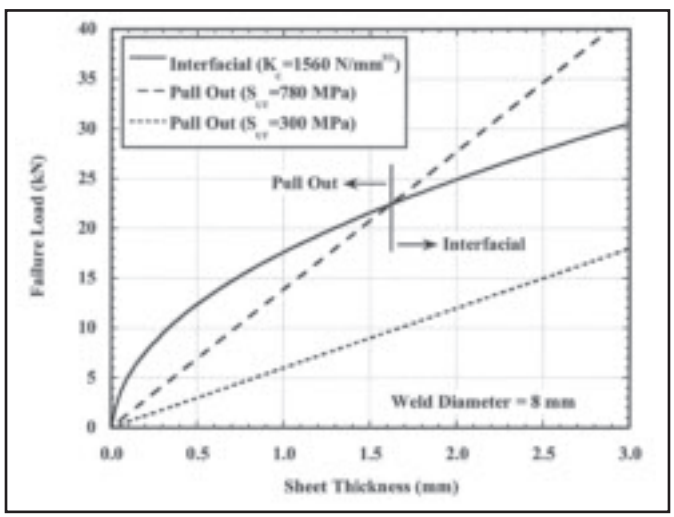

Fig. 13 — Predicted competition between failure modes in the shear-tension test.

in each case. The first two samples listed failed via button pullout and the model-predicted failure loads were in good agreement with the actual loads. The following three samples in the table failed via interfacial fracture. For these cases, the model-predicted loads for pullout failure are listed. The interesting results shown here are that, although interfacial fracture occurred in the samples, the load-carrying capacity of the weld was greater than 90% of the predicted failure load if pullout had occurred. This indicates that the load-bearing capacity of these welds was not significantly affected by the fracture mode. Therefore, the mode of failure should not be the only criteria used to judge the quality of spot welds. The load-bearing capacity of the weld should be the primary focus in the evaluation of the shear-tension test results in AHSS.

In order to get an estimate of the load required for interfacial fracture in the shear-tension test, the stress intensity in Equation 3 was set equal to the fracture toughness of the material and the load was solved for. This is shown in Equation 4 where F_{IF} is the load to cause interfacial fracture of the weld, and K_C is the fracture toughness of the material. The fracture toughness describes the ability of a material to carry load in the presence of a flaw and is determined from testing. Generally, ductile materials tend to have high fracture toughness while the opposite is true for brittle materials. Based on the work done by Zhang (Ref. 9), Equation 4 (rather than Equation 2) was thought to better represent the parameters governing the interfacial fracture mode. The previously determined load to cause pullout failure (Equation 1) was, however, considered to be appropriate. The predicted relationship for pullout load likely agreed well with the measured data because this failure initiates in the form of necking in the base metal near the weld heat-affected zone as opposed to at the notch radius around the perimeter of the weld nugget.

Equations 1 and 4 are plotted graphically in Fig. 13. In this plot, the weld diameter was assumed to be constant at 8 mm and the tensile strength assumed was the minimum allowable for this grade (780

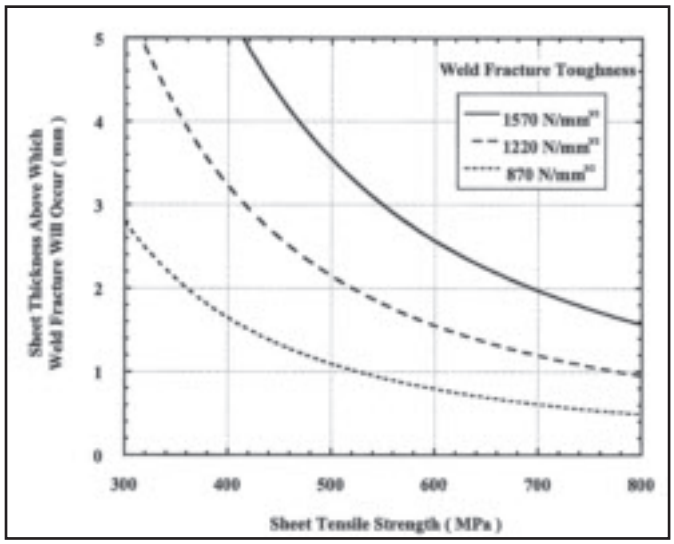

Fig. 14 — Sheet thickness above which interfacial fracture is predicted to occur as a function of sheet tensile strength and the fracture toughness of the weld.

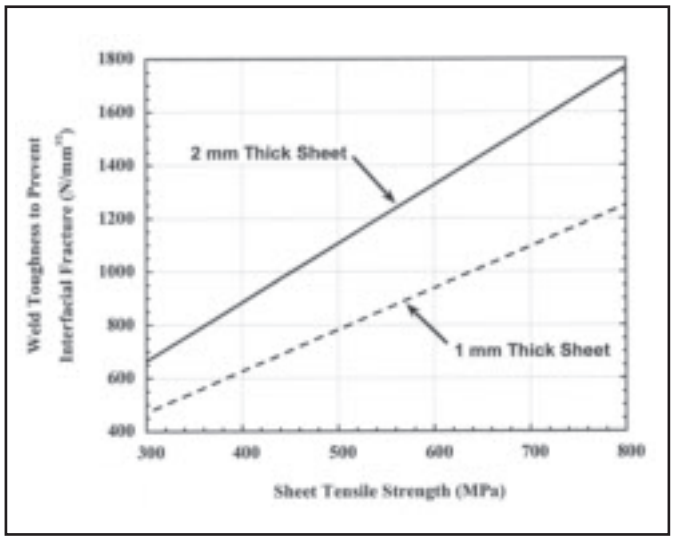

Fig. 15 — Predicted weld toughness required to avoid interfacial fracture in the shear-tension test as a function of sheet tensile strength for 1- and 2-mm-thick sheets.

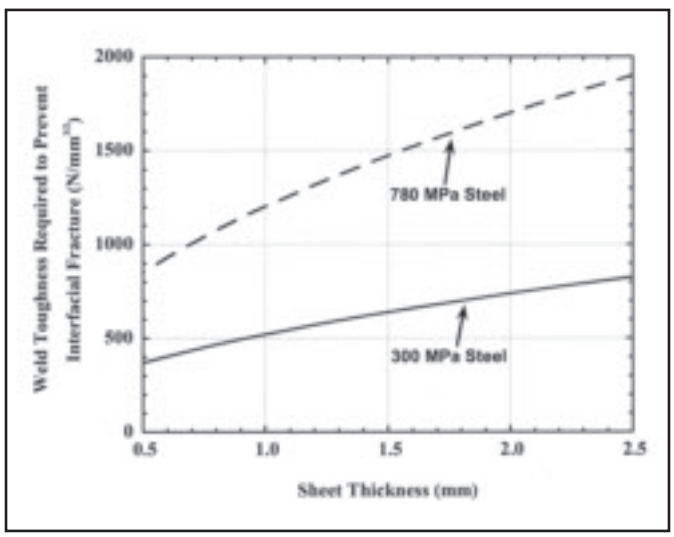

Fig. 16 — Predicted weld toughness required to avoid interfacial fracture in the shear-tension test as a function of sheet thickness and tensile strength.

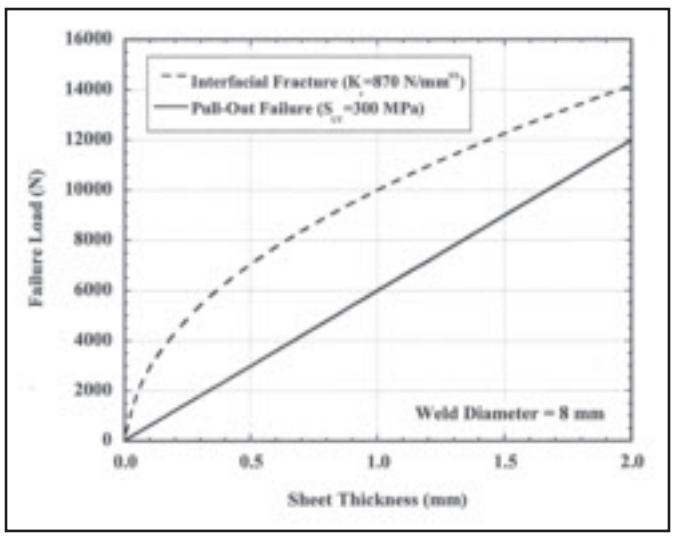

Fig. 17 — Predicted failure load as a function of sheet thickness for a low-strength steel having a weld with poor load-carrying capacity. For a low-strength sheet, a pullout failure is predicted even when the load-carrying capacity of the weld is poor.

MPa), and the failure load is plotted as a function of sheet thickness. The interfacial fracture load is plotted assuming a fracture toughness of 1560 N/mm$^{3/2}$, and the pullout failure load is plotted for a low-strength steel (300 MPa) and a higher-strength steel (780 MPa). For the curve representing the low-strength steel, the predicted pullout failure load is less than the interfacial fracture load over this entire range of sheet thickness. This indicates that pullout failure will occur in every case. For the higher-strength sample, the curve for pullout failure and interfacial fracture intersect at a sheet thickness of 1.6 mm. This indicates that for the high-strength sheet sample, interfacial fracture will be the expected failure mode for sheet thicknesses greater than 1.6 mm.

The critical parameters that control the transition between failure modes can be determined by setting Equation 4 equal to Equation 1. Some of these results are shown in the last four figures. Figure 14 shows that critical sheet thickness above which interfacial fracture will occur becomes less as the strength of the sheet increases. Thus, for higher-strength sheet, interfacial fracture can become the expected failure mode in thicker samples. Figure 15 shows the fracture toughness of the weld required to maintain pullout failures increases with the strength of the sheet indicating that interfacial fractures are more likely to occur with high-strength steels. Figure 16 shows that the weld toughness required to maintain pullout failures also increases with sheet thickness. Figure 17 shows the predicted pullout and interfacial failure loads for a low-strength steel shear-tension test sample that has a weld with poor load-carrying capacity. The failure load required for pullout is less than that for interfacial fracture over the entire range of sheet thickness

shown in the plot. This indicates that for low-strength steels, a full button pullout failure could be expected even for the case where the weld has poor load-carrying capacity. For high-strength steels, however, this was not found to be the case. Interfacial fracture was predicted to occur for cases where the weld has superior fracture toughness and high load-carrying capacity. These predictions shown in Figs. 15–17 agree well with known characteristics of spot welds.

Conclusions

An analysis was performed in which a combination of finite element modeling and fracture mechanics calculations was used to predict the weld failure modes in the shear-tension tests of resistance spot welds in AHSS grades. In the finite element model, the base material and heat-affected zone and weld properties were assumed to be homogeneous. The homogeneous model predictions agreed well with the test data for cases where pullout failures occurred. This is because the pullout failures most often initiated in the base metal outside of the notch at the perimeter of the weld. However, when comparing the homogeneous model results to actual test data, the predicted failure loads for the interfacial fractures were not consistent. For the case of the interfacial failure mode, a relationship was found in the literature to estimate the stress intensity at the weld notch tip. This relationship was used along with the equation developed for the pullout failure to define variables that affect the failure mode and load for the shear-tension test.

The results of the analyses showed the following:

1. The mathematical equation derived based on the finite element modeling showed that the force required to cause a button pullout fracture was found to be proportional to the tensile strength of the sheet as well as the diameter of the weld and the thickness of the sheet.

2. The present analyses showed that, for low-strength steels (tensile strength less than or equal to 300 MPa), a full button pullout could occur even when welds have a poor load-carrying capacity. For high-strength steels, however, this was not found to be the case. Interfacial fracture was predicted to occur in the shear tension test for cases where the weld has superior fracture toughness and high load-carrying capacity.

3. It was determined that there is a critical sheet thickness above which the expected failure mode could move from pullout to interfacial fracture. It was shown that, as the strength of the sheet increases, the fracture toughness of the weld required to avoid interfacial fractures must also increase. In the higher-strength, less-ductile steels, this is not likely to occur and interfacial fracture could become the expected failure mode.

4. The load-carrying capacity of the samples that failed via interfacial fracture was found to be more than 90% of the maximum load associated with the full button pullout. This indicates that the load-bearing capacity of these welds is not significantly affected by the fracture mode. Thus, the mode of failure should not be the only criteria used to judge the results of the shear-tension test. The load-carrying capacity of the weld should be considered the most important parameter when evaluating the shear-tension test results in AHSS.

References

1. Schultz, R. A. 2007. Metallic material trends for North American light vehicles. Paper presented at the Great Designs in Steel Seminar, American Iron and Steel Institute, Southfield, Mich.

2. Horvath, C. 2007. Material challenges facing the automotive and steel industries from globalization. Paper presented at the Great Designs in Steel Seminar, American Iron and Steel Institute, Southfield, Mich.

3. D8.9M-2002, *Recommended Practices for Test Methods for Evaluating the Resistance Spot Welding Behavior of Automotive Sheet Steel Materials*. Miami, Fla.: American Welding Society.

4. Davidson, J. A. 1983. Design-related methodology to determine the fatigue life and related failure mode of spot-welded sheet steels. International Conf. on Technology and Applications of High-Strength Low-Alloy Steels, ASM International Technical Series 8306-022, Metals Park, Ohio.

5. Davidson, J. A., Imhof, E. J. Jr., 1984. *The Effect of Tensile Strength on the Fatigue Life of Spot-Welded Sheet Steels*. SAE Technical Paper No. 848110.

6. Davidson, J. A., and Imhof, E. J. 1983. *A Fracture Mechanics and System-Stiffness Approach to Fatigue Performance of Spot-Welded Sheets.* SAE Technical Paper No. 830034.

7. Pook, L. P. 1975. Fracture mechanics analysis of the fatigue behavior of spot welds. *International Journal of Fracture* Vol. 11, pp. 173–176.

8. Chao, Y. J. 2003. Ultimate strength and failure mechanism of resistance spot weld subjected to tensile, shear, or combined tensile/shearloads. *Journal of Engineering Materials and Technology* Vol. 125(4): 125–132.

9. Radaj, D., and Zhang, S. 1991. Simplified formulae for stress intensity factors of spot welds. *Engineering Fracture Mechanics* Vol. 40(1): 233–236.

10. Zhang, S. 1997. Stress intensities at spot welds. *International Journal of Fracture* Vol. 88, pp. 167–185.

11. Rege, J. S., Inazumi, T., Nagataki, T., Smith, G., Zudeima, B., and Denner, S. 2002. Development of HDGI/HDGA DP steel family at National Steel Corp. *44th MWSP Conference Proceedings*, ISS, Vol. XL.

12. Mahieu, J., Maki, J., Claessens, S., and De Cooman, B. C. 2001. Hot dip galvanizing of Al alloyed TRIP steels. 43rd MWSP Conference Proceedings, ISS, Vol. XXXIX.

13. Tumuluru, M. 2006. An overview of the resistance spot welding of coated high-strength dual-phase steels. *Welding Journal* 85(8): 31–37.

Nominees Solicited for Prof. Koichi Masubuchi Award

November 3, 2008, is the deadline for submiting nominations for the 2009 Prof. Koichi Masubuchi Award, sponsored by the Dept. of Ocean Engineering at Massacuusetts Institute of Technology. It is presented each year to one person who has made significant contributions to the advancement of materials joining through research and development. The candidate must be 40 years old or younger, may live anywhere in the world, and need not be an AWS member. The nominations should be prepared by someone familar with the research background of the candidate. Include a résumé listing background, experience, publications, honors, awards, plus a least three letters of recommendation from researchers.

This award was established to recognize Prof. Koichi Masubuchi for his numerous contributions to the advancement of the science and technoogy of welding, especially in the fields of fabricating marine and outer space structures.

Submit your nominations to Prof. John DuPont at *jnd@lehigh.edu.*